ISBN: 978-3-95450-132-8 doi:10.18429/JACoW-IPAC2014-TUPRO077

AGS SNAKE STORIES*

F. Méot, Y. Dutheil, R. Gupta, H. Huang, N. Tsoupas
BNL, Upton, NY, USA
J. Takano, J-PARC, KEK & JAEA, Ibaraki-ken, Japan

Abstract

The fields, particle motion, and spin precession in the AGS snakes have been re-visited. These investigations include re-computation of 3-D OPERA field maps of the snakes and use stepwise ray-tracing tools and methods. There is a series of sub-products of this study, amongst others, the transport of the spin stable axis from AGS to RHIC X and Y kicker exit, cold snake settings for polarized helion programs, high accuracy 3-D field maps in view of long-term motion and spin tracking in the AGS for accurate beam polarization simulations.

INTRODUCTION

The role of the two helical snakes in the AGS is to z-rotate the spin at each passage, by an angle $\phi \approx 10-12$ degrees, warm snake case, or $\phi \approx 20-28$ degrees, cold snake, proton case (about twice as much for helion). This allows overcoming depolarizing resonances, of both imperfection type Q_{sp} = integer, and vertical intrinsic type $Q_{sp} \pm Q_y$ = integer according to the following principles :

Under the effect of the snakes during the acceleration cycle, spins undergo resonant flipping each time the spin tune satisfies Q_{sp} =integer (41 times, from $G\gamma = 4.5$ at injection to 45.5 at extraction), whereas placing the vertical betatron tune Q_y in the forbidden spin tune gap $integer \pm \phi/2\pi$, as resulting from $\cos \pi Q_{sp} = \cos \frac{\phi}{2} \cos \pi G\gamma$, eliminates vertical intrinsic resonances. Non-linear snake resonances $Q_{sp} \pm l Q_y$ = integer, $l \geq 2$, present in the spin tune forbidden gap, are avoided by adjusting Q_y with a margin that depends on the strength of the neighboring linear resonance.

On the other hand the stable spin precession direction $\vec{n}_0$ is in general at a (small) angle to the vertical around the ring. This drives horizontal intrinsic spin resonances, $Q_{sp} \pm Q_x$ = integer, their effect is minimized by 80 local tune jumps, using a pair of fast quadrupoles. AGS optics in addition includes coupling sources (e.g., main magnet defects, the snakes themselves at low energy), which also excite resonances $Q_{sp} \pm Q_x$ = integer.

The extraction $G\gamma$ value ($G\gamma = 45.5$ in recent RHIC polarized proton runs) is chosen at the optimum match between the periodic $\vec{n}_0$ at the extraction septum H10 in the AGS, and the vertical periodic $\vec{n}_0$ at the injection kicker in RHIC. The transport from the former to the latter is ensured by the AtR (AGS to RHIC), a non-planar beam line.

Thus, accurate control of beam polarization in the AGS, of its transport along the acceleration cycle, and of its delivery, the closest possible to vertical, at RHIC-Blue and RHIC-Yellow injection kickers, require an accurate knowledge of the snake fields and of their settings.

Details regarding the present study, including Helion conditions, can be found in Ref. [1].

ORBIT, OPTICS, SPIN MOTION

Warm Snake

The AGS warm snake, installed in 2004 [2], located in the E20 straight section, is a normal conducting helical dipole with double pitch structure (0.4/0.195/0.4 deg/m over 0.39/1.32/0.39 m, entrance/body/exit) designed to ensure minimized orbit defect [3].

The same 3-D OPERA field map as investigated in Ref. [4] is used here. It was computed for the nominal operation conditions, namely, 1.53 T field modulus at the center of the magnet, 2540 Amp coil current.

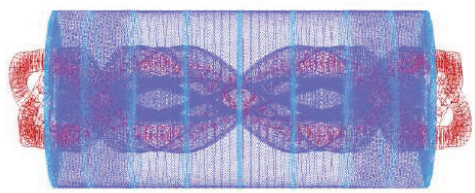

Figure 1: 3-D OPERA model of the warm snake [2].

Spin tracking data, as obtained from ray-tracing, are detailed in Figs. 2 and 3. The spin precession is interpolated at better than $2\,10^{-3}$ accuracy (relative to actual tracking outcomes) from $G\gamma = 4.5$ and beyond, and with B in the vicinity of B_0, by, see Fig. 3,

$$\mu(B, G\gamma) = \left(\frac{B}{B_0}\right)^2 \left[C_0 + \frac{C_1}{G\gamma} + \frac{C_2}{(G\gamma)^2}\right] \qquad (1)$$

with $B_0 = 1.5333$ Tesla, $C_0 = 10.578$, $C_1 = -1.284$, $C_2 = 34.60$. Checking data from earlier studies [4] was part of the motivations for the present work, discrepancies have been found, see Ref. [1] for details.

The helix radius in the warm snake is approximated at a few percent level of accuracy, in $G\gamma \in [4.5, 50]$, and with B in the vicinity of B_0, by

$$r(B, G\gamma)[m] = \frac{B}{B_0}\frac{C}{G\gamma}, \quad C \approx 85 \qquad (2)$$

The first order mapping of the snake on the other hand, is rigidity dependent. It can be computed from particle trajectories taken paraxial to the $G\gamma$-dependent helical orbits

* Work supported by Brookhaven Science Associates, LLC under Contract No. DE-AC02-98CH10886 with the U.S. Department of Energy.

ISBN: 978-3-95450-132-8 doi:10.18429/JACoW-IPAC2014-TUPRO077

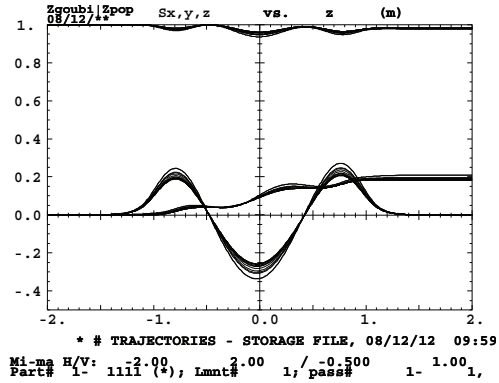

Figure 2: Spin components along helical orbits, projections of a z-rotation.

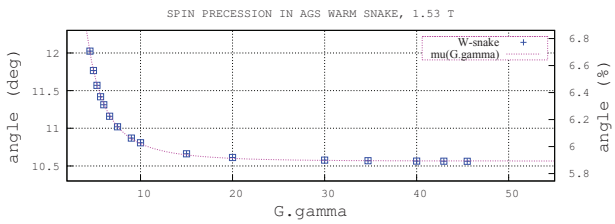

Figure 3: Spin precession angle in the warm snake, at various $G\gamma$ values, and interpolation function with truncated B0, C0-C2 data of Eq. 1.

across the magnet. By contrast with spin precession results, today's particle optics data come out to be in good agreement with those established in detail in Ref. [4] and used in the MADX model of the AGS [5].

Cold Snake

The AGS cold snake, installed in 2005 and first operated in 2006 [6, 7], is located in the A20 straight section in the AGS. It is a super-conducting helical dipole with double pitch structure (0.392/0.2053/0.392 deg/mm over 0.393/1.154/0.393 m, entrance/body/exit), which ensures minimized orbit defect. The device includes a 0.82 m long solenoid winding aimed at cancelling the longitudinal field integral $\int B_z\, ds$ experienced by the particles on the helical orbit, at $G\gamma = 9$. It also includes a 0.3 m long, 0.008 T.m, vertical corrector at both ends.

It was realized in the course of the present study that, instead of the 152 Amp solenoid current value used up to

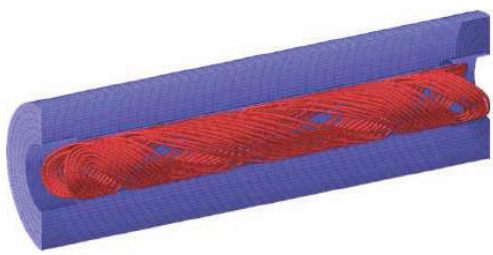

Figure 4: 3-D model of the cold snake, OPERA simulation.

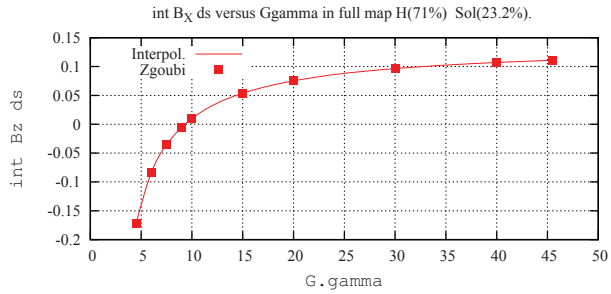

Figure 5: Integral of longitudinal field component along the orbit, it vanishes at $G\gamma \approx 9$. Square markers from Zgoubi tracking and interpolating spline (solid line).

now, the compensation solenoid setting should instead be 75 Amp about with the 68.2% helix setting (238 A). Orbit and spin tracking data in the case of a 81 Amp current in the solenoid (71% helix field map is used), which has the property of cancelling $\int B_z\, ds$ at $G\gamma = 9$, see Fig. 5 (rigidity 15.396 T.m, helix radius 1.08 cm), are detailed in Figs. 6 and 7. It can be observed that such change in solenoid current is not innocent in terms of snake strength, it changes the spin precession by a sensible amount, larger at lower energy.

The spin precession is interpolated at better than $3\,10^{-3}$ accuracy (relative to actual tracking outcomes) from $G\gamma = 4.5$ and beyond, and with B in the vicinity of B_0, by, Fig. 7,

$$\mu(B, G\gamma) = \left(\frac{B}{B_0}\right)^2 \left[C_0 + \frac{C_1}{G\gamma} + \frac{C_2}{(G\gamma)^2} + \frac{C_3}{(G\gamma)^3}\right] \quad (3)$$

with $B_0 = 2.2588$ Tesla, $C_0 = 20.163$, $C_1 = 11.997$, $C_2 = 40.61$, $C_3 = 99.1$.

The helix radius in the 71% helix snake is approximated at a few percent level of accuracy, in $G\gamma \in [4.5, 50]$ range and with B in the vicinity of B_0, by

$$r(B, G\gamma)[m] = \frac{B}{B_0}\frac{C}{G\gamma}, \qquad C \approx 100 \quad (4)$$

Tracking shows that the linear dependence in B is however very accurate (notwithstanding any saturation effect, *i.e.*, simply scaling the field map data), in the case of the zero solenoidal field snake, over the all range $B[T] \in [0, 3]$.

The first order mapping of the snake is rigidity dependent. It comes out to be quite close to that used in the MADX model of the AGS [5].

Linear Combination of Helix and Solenoid 3-D Field Maps

During the present studies regarding the cold snake it has been verified and investigated further that the magnetic field in the useful region in the snake, in the case of solenoid field in 80~150 Amp range, can be obtained by a linear combination of the helix and solenoid field maps computed independently, given a small correction on the field amplitude : the combined map has to be multiplied by 1.016, in order to get agreement on spin precession with full map field, at better than 0.6%, over the $G\gamma$: $4.5 \rightarrow 50$ range, proton.

ISBN: 978-3-95450-132-8 doi:10.18429/JACoW-IPAC2014-TUPRO077

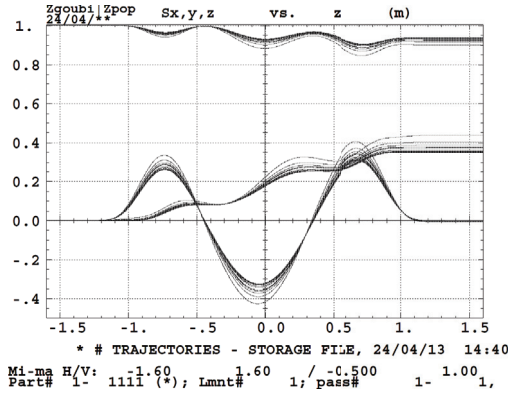

Figure 6: Spin components along helical orbits, projections of a z-rotation.

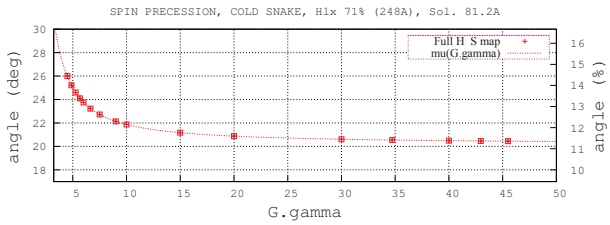

Figure 7: Value of spin precession angle in the cold snake, 71% helix and 81 Amp solenoid current, at various $G\gamma$ values, and interpolation function with truncated B0, C0-C3 data of Eq. 3.

That combination appears to apply over a large range of helix and solenoid fields, including regular polarized proton settings and the substantially different polarized helion settings [1].

IMAGE IN RHIC OF AGS $\vec{n}_0$ SPIN VECTOR

The results obtained so far, regarding the transport of $\vec{n}_0$ from the AGS H10 extraction septum to RHIC Blue and Yellow injection kickers via the AtR line, are summarized here. They confirm the validity of the choice for the AGS extraction energy in the latest RHIC runs, $G\gamma = 45.5$.

The cold snake follows earlier RHIC run settings, namely, using a linear combination of 68.2% helix (238 A for a maximum 350 A) and 21.6% solenoid (~76 A for a 350 A maximum).

The results are schemed in Fig. 8 which displays the vertical projection of the stable spin direction, as obtained from stepwise ray-tracing through the AtR, at three different locations : H10 septum in the AGS, RHIC Blue ring injection kicker, RHIC Yellow ring injection kicker.

Details concerning this study can be found in Ref. [8].

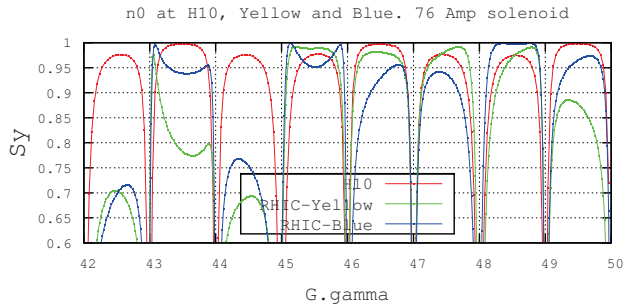

Figure 8: Vertical component of the stable spin direction, $\vec{n}_0$, as a function of $G\gamma$, as observed at H10 extraction septum in the AGS, at RHIC-Blue and at RHIC-Yellow injection kickers. Snake settings : 68.2% helix, 21.6% solenoid fields.

AGS PP OPTIMIZATION

High accuracy 3-D field maps of the warm and cold snakes have been produced for this study. They also have a longer extent than the original maps, so to fully encompass the fall-off regions at snakes ends. Based on these, tracking of polarized beams over full AGS cycles (150000 turns about) can be performed, for the purpose of optics and polarization studies and optimization. The low energy region of the cycle (below transition), where the snake have a strong effect on the optics, is addressed in particular in a companion paper [9].

REFERENCES

[1] F. Méot, R. Gupta, H. Huang, N. Tsoupas, Where are the AGS snakes?, BNL C-AD Tech. Note C-A/AP/485 (2013).

[2] J. Takano et al., Field measurements in the AGS warm snake, WEPLT114, Procs. EPAC 2004 Acc. Conf., Lucerne.

[3] T. Roser, et al., Helical partial snake for the AGS, RHIC Tech. Note SN072, March 17, 1998.

[4] A. Luccio et al., Tracking through a warm helical snake for the AGS, C-A/AP/136 (2004).

[5] V. Schoefer et al., RHIC injector complex online model status and plans, FR5REP003, Proc. PAC09 Acc. Conf., Vancouver.

[6] E. Willen et al., Superconducting helical snake magnet for the AGS, MPPT046, Procs. PAC 2005 Acc. Conf., Knoxville.

[7] R. Gupta et al., Magnetic design of a superconducting AGS snake, WPAE002, Procs. PAC 2003 Conf., Portland.

[8] F. Méot, H. Huang, N. Tsoupas, On the image in RHIC of AGS n0, via the AtR BNL C-AD Tech. Note C-A/AP/502 (2013).

[9] Y. Dutheil et al., Optimization of the polarized proton AGS Zgoubi Model in the Injection Energy Range, THPRO088, these proceedings, IPAC 2014, Dresden, Germany (2014).